1-20-2016

Hyperfine Rather Than Spin Splittings Dominate the Fine Structure of the $B\,^4\Sigma^- – X\,^4\Sigma^-$ Bands of AlC

Dennis J. Clouthier
University of Kentucky, dclaser@uky.edu

Aimable Kalume
University of Kentucky, aimable.kalume@uky.edu

Hyperfine Rather Than Spin Splittings Dominate the Fine Structure of the $B\,^4\Sigma^- – X\,^4\Sigma^-$ Bands of AlC

Notes/Citation Information
Published in *The Journal of Chemical Physics*, v. 144, issue 3, 034305, p. 1-8.

The following article appeared in *The Journal of Chemical Physics* 144, 034305 (2016) and may be found at https://doi.org/10.1063/1.4939797.

Digital Object Identifier (DOI)
https://doi.org/10.1063/1.4939797

Hyperfine rather than spin splittings dominate the fine structure of the B $^4\Sigma^-$–X $^4\Sigma^-$ bands of AlC

Dennis J. Clouthier, and Aimable Kalume

Citation: The Journal of Chemical Physics **144**, 034305 (2016);
View online: https://doi.org/10.1063/1.4939797
View Table of Contents: http://aip.scitation.org/toc/jcp/144/3
Published by the American Institute of Physics

Hyperfine rather than spin splittings dominate the fine structure of the $B\,^4\Sigma^-$–$X\,^4\Sigma^-$ bands of AlC

Dennis J. Clouthier[a] and Aimable Kalume
Department of Chemistry, University of Kentucky, Lexington, Kentucky 40506-0055, USA

(Received 3 December 2015; accepted 30 December 2015; published online 20 January 2016)

Laser-induced fluorescence and wavelength resolved emission spectra of the $B\,^4\Sigma^-$–$X\,^4\Sigma^-$ band system of the gas phase cold aluminum carbide free radical have been obtained using the pulsed discharge jet technique. The radical was produced by electron bombardment of a precursor mixture of trimethylaluminum in high pressure argon. High resolution spectra show that each rotational line of the 0-0 and 1-1 bands of AlC is split into at least three components, with very similar splittings and intensities in both the *P*- and *R*-branches. The observed structure was reproduced by assuming $b_{\beta S}$ magnetic hyperfine coupling in the excited state, due to a substantial Fermi contact interaction of the unpaired electron in the aluminum 3*s* orbital. Rotational analysis has yielded ground and excited state equilibrium bond lengths in good agreement with the literature and our own *ab initio* values. Small discrepancies in the calculated intensities of the hyperfine lines suggest that the upper state spin-spin constant λ′ is of the order of ≈0.025–0.030 cm^{-1}. © *2016 AIP Publishing LLC.* [http://dx.doi.org/10.1063/1.4939797]

I. INTRODUCTION

Solid phase aluminum carbide, prepared by the reaction of aluminum and carbon in an electric arc furnace and commercially available, has the formula Al_4C_3 and is a thermally stable yellow to brown crystalline material that reacts with water to produce methane and $Al(OH)_3$. Aluminum carbides have a variety of applications in refractory materials, in thermally conductive ceramics, and in the preparation of new materials.

In sharp contrast, the diatomic molecule AlC is highly reactive, little known, and has only been observed experimentally in a few instances. Despite these limitations, it is of considerable interest, especially in the context of interstellar molecules. Silicon carbides are uncommonly plentiful in space, both as small molecules,[1–4] such as SiC, the ring compounds SiC_2 and SiC_3, and the linear chain SiC_4, and as the major constituents of grains and dust around carbon-rich stars.[5] Aluminum is the 12th most abundant element in space and the small molecules AlF, AlCl, AlO, AlOH, and AlNC have been found[6–10] in various circumstellar environments. Since carbon is also very abundant, especially in the atmospheres of carbon-rich stars, it has been suggested that AlC may be of astrophysical interest,[11] although the micro/millimeter wave spectrum has never been reported. In the present work, we have analyzed high resolution spectra of two electronic bands of AlC, which provide constants that should be useful in searches for the rotational spectra.

An early (1954) report[12] of the possible observation of AlC emission from a King furnace source was later shown to be due to Al_2.[13] In 1990, Knight and co-workers[14] reported the observation of the electron spin resonance (ESR) spectrum of $Al^{12}C$ and $Al^{13}C$ produced by laser vaporization of Al_4C_3 and trapping in neon or argon matrices. The ESR data were consistent with AlC having a $^4\Sigma$ ground state with the valence configuration $\ldots\sigma^1\pi_x^1\pi_y^1$ and the three unpaired electrons residing primarily on the carbon atom. In 1993, Brazier[15] published data on the $B\,^4\Sigma^-$–$X\,^4\Sigma^-$ emission spectrum of gas phase AlC obtained from a composite Al_4C_3/Al hollow cathode source. The band system near 22 000 cm^{-1} consisted of a series of weak bands extending up to v′ = 6 and down to v″ = 7. Four bands were rotationally analyzed yielding r_e'' = 1.955 03 Å and r_e' = 1.894 16 Å. The spin splittings were only partially resolved and did not allow an accurate determination of the signs or magnitudes of the spin-spin parameters in the combining states. Contemporaneously, Thoma *et al.*[11] observed the same transition of AlC in an argon matrix in both absorption and laser-induced fluorescence (LIF). In 1994, Chertihin, Andrews, and Taylor[16] reported the argon matrix infrared spectra of $Al^{12}C$ and $Al^{13}C$ obtained from the reaction of pulsed laser evaporated Al and C atoms. Most recently, in 2009, Brazier and Tandoc[17] reported a further study of the emission spectrum of AlC in which a corona excited supersonic expansion source was used to obtain low temperature spectra. The original analysis of the $B\,^4\Sigma^-$–$X\,^4\Sigma^-$ system was confirmed and numerous bands of the previously unknown low-lying $A\,^4\Pi$–$X\,^4\Sigma^-$ system were observed and analyzed.

The aluminum carbide diatomic molecule has been the subject of many theoretical papers,[18–26] culminating in two very thorough studies of the ground[25] and numerous excited states.[26]

II. EXPERIMENT

The jet-cooled AlC radical was produced by electron bombardment of a precursor mixture of the room temperature

[a]Author to whom correspondence should be addressed. Electronic mail: dclaser@uky.edu

vapor (11–12 Torr) of trimethylaluminum in 40 psi of argon in a pulsed discharge jet apparatus.[27] The gas mixture was prepared by flowing argon over the surface of liquid trimethylaluminum held in a Pyrex U-tube and injected into the vacuum chamber through a molecular beam valve (General Valve, series 9). After a suitable time delay, a pulsed DC discharge was struck between a pair of stainless steel ring electrodes mounted in a cylindrical Delrin flow channel attached to the end of the pulsed valve. The discharge fragmented the precursor molecules and subsequent reactions in the flow channel prior to supersonic expansion generated the AlC species. A small reheat tube[28] attached to the end of the flow channel was found to enhance the production of AlC and suppress the background glow from excited state argon atoms produced in the discharge.

For low-resolution LIF experiments, the radicals were interrogated 1 cm downstream of the reheat tube with the collimated beam of a pulsed tunable dye laser (Lambda Physik Scanmate 2E, linewidth 0.1 cm^{-1}) and the resulting fluorescence imaged through appropriate cutoff filters onto the photocathode of a high gain photomultiplier (EMI 9816QB). The pulsed fluorescence signals were processed with a gated integrator and recorded on a LabVIEW based data acquisition system of our own design. The spectra were calibrated to an estimated accuracy of 0.1 cm^{-1} with optogalvanic lines from neon- and argon-filled hollow cathode lamps.

We found that the LIF signals were often contaminated by lines of other fluorescent species, which masked the weaker features. To overcome this problem, we used a synchronous scanning LIF (sync-scan LIF) method of detection[29] in which our emission monochromator (Spex 500M), tuned to a particular emission feature, was used as a narrow bandpass filter. As the LIF laser was scanned, the monochromator, offset to lower frequency by the equivalent of an AlC ground state vibrational interval, was scanned synchronously under computer control, so that only those absorption features, which emitted down to the chosen vibrational level, were detected. Spectra recorded in this fashion had a much better signal-to-noise ratio and fewer impurity lines.

High resolution (0.035 cm^{-1}) sync-scan LIF spectra of the 0-0 and 1-1 bands were recorded with the same apparatus, with an angle-tuned etalon inserted in the cavity of the dye laser. The spectra were calibrated to an estimated accuracy of 0.003 cm^{-1} using $^{130}Te_2$ LIF lines.[30]

Single vibronic level emission spectra were obtained by tuning the LIF laser to a strong rotational line of a particular band and focusing the resulting fluorescence with an $f/1.5$ lens system onto the entrance slit of a 0.5 m scanning monochromator (Spex 500M). The pulsed fluorescence signals were detected with a red-sensitive photomultiplier (RCA C31034A), amplified by a factor of 800, sampled with a gated integrator, and recorded digitally. The emission spectra were calibrated to an accuracy of ±2 cm^{-1} using emission lines from an argon discharge lamp. A 1800 line/mm grating blazed at 400 nm was employed in this work, with a bandpass of 0.1-0.5 nm, depending on the strength of the dispersed fluorescence signal.

III. THEORETICAL CALCULATIONS

As an aid to understanding the spectra, we have undertaken a limited number of theoretical calculations of the properties of the ground state ($X\,^4\Sigma^-$) of aluminum carbide, primarily to provide estimates of molecular constants not currently available in the literature. We performed a series of density functional theory (DFT) calculations using the GAUSSIAN 09 program suite[31] with the Becke three parameter hybrid density functional[32] with the Lee, Yang, and Parr (B3LYP) correlation functional[33] and Dunning's correlation consistent basis sets[34] augmented by diffuse functions (aug-cc-pVTZ, aug-cc-pVQZ, and aug-cc-pV5Z). For the aluminum atom, the basis sets were the same except that we have used the reoptimized versions with an additional tight d function (aug-cc-pV(T+d)Z, etc.).[35] The bond length was optimized, the vibrational frequency calculated, and the aluminum hyperfine and electronic spin-rotation parameters were predicted. Our own unpublished tests of the B3LYP method with these basis sets suggest that it gives fairly reliable

TABLE I. Calculated molecular parameters (cm^{-1}) for the ground state of AlC.

	This work	Other work	
Parameter	B3LYP aug-cc-pV(5+d)Z	Reference 22 B3LYP/aug-cc-pVTZ	Reference 25 MRCI/aug-cc-pVQZ
r_e (Å)	1.9687	1.976	1.971
ω_e (cm^{-1})	626.2	622	654.2
$\omega_e x_e$ (cm^{-1})	...	3.629	6.76
B_e (cm^{-1})	0.5241	0.516	
D_e (cm^{-1})	...	1.418×10^{-6}	1.33×10^{-6}
α_e (cm^{-1})	...	4.24×10^{-3}	4.5×10^{-3}
Isotropic Fermi contact b_F (Al) (cm^{-1})	−0.0015[a]		
Nuclear quadrupole χ_{aa} (Al) (cm^{-1})	−0.001		
Electron spin-rotation γ (cm^{-1})	0.014[a]		
Electron spin-spin λ (cm^{-1})	0.006[b]		
Dipole moment (D)	2.00		

[a]The values calculated from the ESR spectrum parameters[14] are $b_F = \pm 0.0008$ cm^{-1} and $\gamma = -0.0011$ cm^{-1}.
[b]Calculated from the ESR zero-field splitting parameter $D = 374$ MHz, Ref. 14.

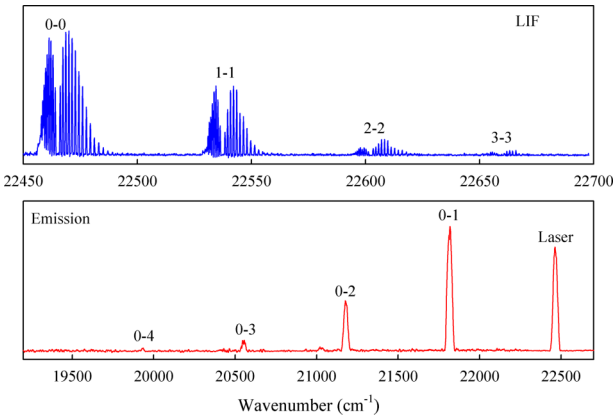

FIG. 1. Survey sync-scan LIF (top) and emission (bottom) spectra of the jet-cooled AlC molecule. The LIF spectrum was recorded by setting the monochromator to detect emission down to v″ = 1 (offset = 650 cm^{-1}) in the ground state. The emission spectrum was obtained by laser excitation of the R(3) rotational line at 22 469.9 cm^{-1}.

predictions of the hyperfine and spin-rotation constants for open shell species containing main group atoms.

We find that most of the molecular parameters show little variation with increasing basis set size from TZ to 5Z. The results of our theoretical studies with the largest basis sets are summarized in Table I, along with the results of previous calculations of similar parameters (where available).

IV. RESULTS AND ANALYSIS

A. Low-resolution LIF and emission spectra

A low resolution sync-scan LIF spectrum of AlC and the corresponding emission spectrum obtained by exciting the R(3) transition of the 0-0 band are shown in Fig. 1. The LIF spectrum shows the 0-0 and 1-1 bands previously analyzed in detail by Brazier[15] along with the new 2-2 and 3-3 sequence bands. These latter two bands do not provide any new information, other than confirming previous assignments, as Brazier[15,17] has already reported the 1-2, 2-3, and 3-4 bands, which encompass the same upper and lower states. We have calculated the positions of the R(0) and P(1) lines of the new 2-2 and 3-3 bands from Brazier's equilibrium constants and it is gratifying that they agree within our measurement error (±0.1 cm^{-1}). The emission spectrum shows a simple progression of bands that can be fitted to the usual anharmonic vibrational formula giving ω_e = 654.0(25) and $\omega_e x_e$ = 5.3(7) cm^{-1} in good agreement with the much more precise constants given in Ref. 17.

B. Rotational analysis of the high resolution spectra of the 0-0 and 1-1 bands

Fig. 2 shows the 0-0 band sync-scan LIF spectrum recorded at our highest resolution (0.035 cm^{-1}), although the linewidths of about 0.055 cm^{-1} suggest that there is some residual power broadening or underlying structure to each feature. It is immediately apparent that each rotational line is split into 3 major fine structure components, with relative intensities from low to high wavenumbers of approximately 1:1.3:1.5 and almost constant intervals of 0.08 cm^{-1} (medium-weak) and 1.1 cm^{-1} (strong-medium). Careful study shows that there is a weaker blended shoulder on the low wavenumber side of many of the triplets. Some of the low-N triplets in Fig. 2, such as $R(1)$, $R(2)$, and $P(4)$ do not follow the usual pattern but instead exhibit a slightly more intense central feature. At least part of this effect is a result of laser and or discharge fluctuations as other spectra taken under similar conditions have comparable intensities for the two highest wavenumber features, but there does seem to be a persistent anomaly. The high resolution spectrum of the 1-1 band (not shown) has essentially the same structure.

Initial simulations of the AlC 0-0 band spectrum using the very convenient graphical PGOPHER program[36] and the published constants[15,17] showed that although the B values and

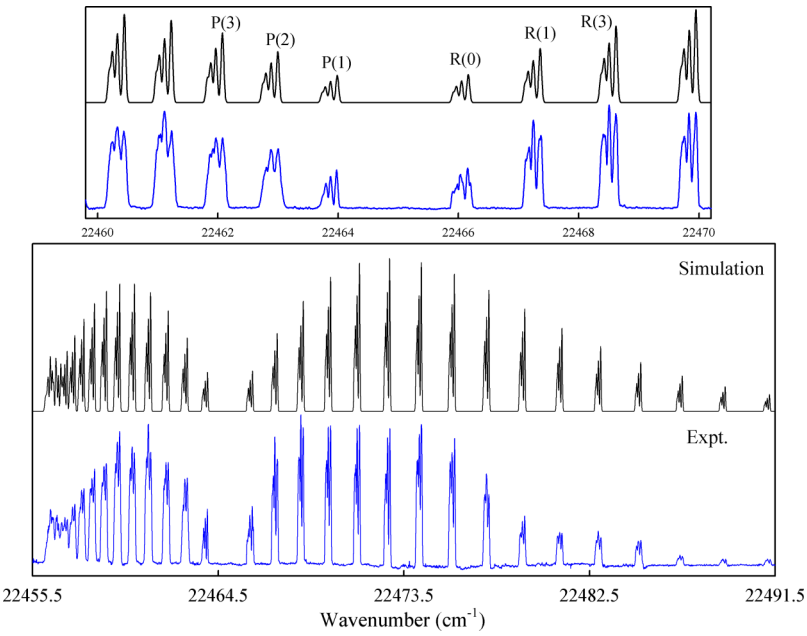

FIG. 2. Observed and calculated high resolution spectra of the 0-0 band of AlC. The experimental spectrum is a composite of three individual etalon scans so the relative intensities across the band are not very reliable. The spectrum was calculated with the constants in Table III, a rotational temperature of 50 K, and a FWHM linewidth of 0.055 cm^{-1}. The upper panel exhibits an expanded region of the band center with rotational assignments showing the resolved fine structure of the individual lines.

TABLE II. AlC effective molecular constants (in cm^{-1}).

	0-0 band		1-1 band	
Constant	This work	Reference 15	This work	Reference 15
B''	0.528 165(61)[a]	0.528 386(65)	0.523 161(75)	0.523 112(75)
T_v	22 464.935 9(12)	22 464.958(4)	22 537.240 1(14)	22 537.290(11)
B'	0.562 300(54)	0.562 561(67)	0.556 070(67)	0.556 072(84)
b_F' (Al)	0.027 95(27)	...	0.027 75(33)	...
#[b]	73	...	67	...
σ (cm^{-1})[c]	0.006 6	...	0.007 7	...

[a]The numbers in parentheses are standard errors of 1σ.
[b]Number of transitions fitted.
[c]Overall standard error of fitting.

band origin were very good, the spin constants $|\lambda'| = 0.08\ cm^{-1}$ and $|\lambda''| = 0.006\ cm^{-1}$ from the ESR spectrum[14] did not satisfactorily reproduce the fine structure. No combination of signs or relative magnitudes yielded the observed triplet fine structure components. Particularly troubling were the $R(0)$ and $P(1)$ lines, which would normally provide direct information about the spin splittings. The former originates in the single $N'' = 0$, $J'' = 1.5$ level of the ground state, so any of the spin splittings must be in the excited state $N' = 1$ level, which can have $J' = 0.5$, 1.5, or 2.5. The converse is true of $P(1)$, which should only exhibit spin-splittings in the lower state. One could envision spin-spin constants of similar magnitude in the two states, which would approximately reproduce the positions of the $P(1)$ and $R(0)$ fine structure lines, but the intensities do not agree with experiment and the higher members of each branch collapse into either singlets or doublets with no evident triplet structure. Various combinations of spin-spin and anomalously large spin-rotation constants alleviated some of these difficulties but almost always gave anomalous intensities and predicted that the $P(1)$ line should have negligible splittings, clearly at odds with experiment.

We subsequently considered the possibility of Al hyperfine effects as the source of the fine structure complications. Our *ab initio* calculations predicted a ground state aluminum ($I = 5/2$) Fermi contact parameter $b_F = -0.0015\ cm^{-1}$, comparable to the $|b_F| = A_{iso} = (A_{//} + 2A_{\perp})/3 \approx 0.0008\ cm^{-1}$ one calculates from the ESR parameters.[14] Similarly, our calculations indicated that the aluminum nuclear quadrupole coupling constant is of the order of $\chi_{aa} = -0.001\ cm^{-1}$. Both of these values are much too small to have any appreciable effect on the spectrum obtained at our resolution. However, Chris Brazier pointed out[37] that the Fermi contact term in the excited state was likely to be much larger as one of the unpaired electrons is nominally in the Al $3s$ orbital and that he had originally speculated that the cause of larger than expected linewidths in his AlC emission spectra was due to excited state hyperfine effects. Armed with this insider information, we readily showed that our spectrum was consistent with a large hyperfine effect in the excited state and negligible spin-spin splittings in both states.

The final constants were obtained in the following manner. The rotational structure was simulated with PGOPHER,[36] fixing all the constants at values of 0.0 except for B'', B', T_0, and the upper state Fermi contact parameter b_F'. The constants were adjusted by hand until the simulation closely matched experiment and then the most intense hyperfine transition in each feature was assigned to the corresponding experimental transition frequency and the constants were adjusted by minimization of the sum of the squares of the obs-calc residuals. For the 0-0 band, 73 individual transitions were fitted with an overall standard deviation of $0.0066\ cm^{-1}$. Although our measurement accuracy is estimated to be $\pm 0.003\ cm^{-1}$, the standard deviation is larger due to the approximately $0.055\ cm^{-1}$ linewidths and the fact that every transition is blended to greater or lesser extent. The four constants were well determined and the simulated spectrum matched experiment very well as shown in Fig. 2. The 1-1 band was fitted in the analogous manner and the resulting constants for both bands are summarized in Table II.

V. DISCUSSION

A. Rotational fine structure

Although the hyperfine coupling scheme used in PGOPHER is $\mathbf{J} = \mathbf{N} + \mathbf{S}$ and $\mathbf{F} = \mathbf{J} + \mathbf{I}$, it is evident from our results that the upper state level pattern must arise from $b_{\beta S}$ coupling[38] in which $\mathbf{G} = \mathbf{I} + \mathbf{S}$ and $\mathbf{F} = \mathbf{N} + \mathbf{G}$. Since the quantum numbers are I = 2.5 and S = 1.5, each upper state rotational level is split into four closely spaced hyperfine components with $G = 4$, 3, 2, or 1 with energies,

$$E_G = 0.5 b_F [G(G+1) - I(I+1) - S(S+1)], \qquad (1)$$

where b_F is the Fermi contact parameter. The energy levels are shown schematically in Fig. 3. At the resolution of our experiment, which implies neglecting spin-spin and hyperfine effects in the ground state, each lower state is characterized by N''. In the excited state, again neglecting spin-spin and hyperfine effects other than the predominant Fermi contact interaction, each N' level has four hyperfine levels whose energies increase with G. Each G level consists of $2G + 1$ degenerate levels labeled by the quantum number F. As shown in Fig. 3, a particular transition from N'' to N' consists of four individual transitions to the four upper state G levels satisfying the overall $\Delta F = 0, \pm 1$ selection rules and the hyperfine splittings and relative intensities are independent of N. Thus, at this level of approximation, the spectrum should consist of a series of rotational lines, each split into four components, with equal splittings and relative intensities

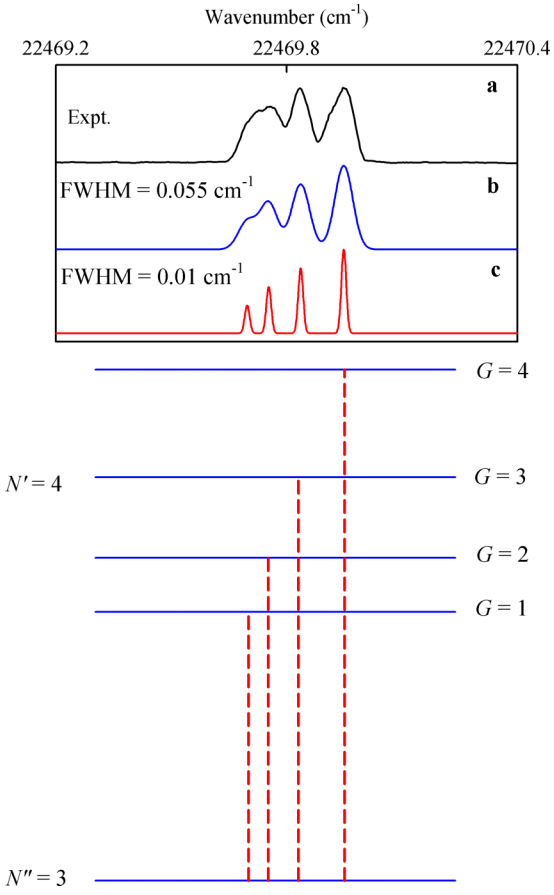

FIG. 3. Experimental (panel **a**) and calculated (panels **b** and **c**) spectra of the 0-0 band R(3) line of AlC (top) and schematic energy levels (bottom). Panel **b** is the calculated spectrum with a linewidth of 0.055 cm^{-1} and panel **c** is the same spectrum calculated with a linewidth of 0.01 cm^{-1} to show the individual transitions. In the energy level diagram, the relative energies of the four components of the $N' = 4$ level are drawn to scale and the transitions (dashed lines) are located to match the spectra.

throughout the branches, as shown in Figs. 2 and 3. This is precisely what is observed experimentally except that the calculated splitting between the $G = 1$ and $G = 2$ components is only 0.056 cm^{-1}, insufficient for them to be resolved, so the transition to the $G' = 1$ level shows up as a slight shoulder on the low wavenumber side of each observed hyperfine triplet of lines.

An alternate method of fitting the lines in the spectrum would be to use the simple energy expression,

$$\Delta\nu = T_0 + B'N'(N'+1) + 0.5b_F[G(G+1) - 12.5] - B''N''(N''+1), \quad (2)$$

where the factor of 12.5 comes from the quantity $I(I+1) - S(S+1)$ with $I = 5/2$ and $S = 3/2$ in Eq. (1). Our least squares results from fitting the observed transitions to Eq. (2) were numerically identical to those obtained with PGOPHER, where the energy levels were obtained by diagonalizing the appropriate matrices. The individual line measurements, assignments (using the G quantum number), and obs-calc residuals are given in Table III.

Although the constants summarized in Table II are probably the best that can be obtained from our spectra, it is clear from an examination of the relative intensities of the lines in the various hyperfine clusters (see Fig. 2 and earlier discussion in Subsection IV B) that there is still a small, persistent discrepancy. As alluded to earlier, the R (1), R (2), and P (4) experimental lines, in particular, exhibit a more intense central feature, contrary to our expectations based solely on hyperfine splittings. It seems natural to attribute these deviations to small spin-spin effects, which are neglected in the present analysis. We have attempted to test this hypothesis in the following manner. First, the ground state spin-spin constant was fixed at the ESR value of ±0.006 cm^{-1} (see Table I). As expected, inclusion of a lower state spin-spin constant of 0.006 cm^{-1} with either signs does not have any perceptible effect on the relative intensities in the calculated spectrum. Then, we tried various values for λ', with the proviso that it does not appreciably perturb the observed three line pattern with a slight shoulder on the low frequency side but redistribute the intensities slightly to better match experiment. It was readily apparent that $\lambda' \approx 0.025$–0.030 cm^{-1} would have the desired effect. Unfortunately, we were unable to fit this constant as all of the calculated splittings are much smaller than our experimental resolution.

One further aspect of the fine structure in the spectrum deserves comment. In previous work,[15] the authors observed that each P- and R-branch line was split into a doublet with a constant separation of 0.14-0.17 cm^{-1} at their resolution of ~0.1 cm^{-1}. When we calculate the spectrum using our constants and a linewidth of 0.1 cm^{-1}, we obtain doublets with the low wavenumber side slightly broader and a branch independent splitting of ~0.13 cm^{-1}, in reasonable accord with their observations. It is only because of our improved resolution that we were able to discern the further splittings that allowed us to understand the hyperfine patterns.

In the course of the present work, we also attempted to record the LIF spectrum of the $A\,^4\Pi$–$X\,^4\Sigma^-$ band system studied by Brazier and Tandoc.[17] These bands are much weaker than those of the B–X transitions and although we were able to detect them with very low S/N ratios, despite considerable effort, we were unable to improve the conditions sufficiently to record high resolution spectra.

B. Molecular constants

The molecular constants obtained from our analyses of the 0-0 and 1-1 bands are compared in Table II to those obtained previously by Brazier.[15] In general, the agreement is very good considering that we used different models to fit the data.

We have used the effective parameters in Table II to calculate the equilibrium molecular constants B_e, α_e, and r_e for the ground and excited states, propagating the errors in the usual manner. The results are collected in Table IV, where they are compared to the previous determinations by Brazier and Tandoc[17] from much more extensive data sets. Considering that the data were very different and the rotational analyses used different constants, the results are in very good agreement. In particular, our equilibrium bond lengths are only 0.0007 Å longer in both states, reflecting our slightly

TABLE III. Observed lines (in cm^{-1}) and assignments of the 0-0 and 1-1 $B\,^4\Sigma^- – X\,^4\Sigma^-$ bands of AlC.

		0-0 band				1-1 band			
N''	G′	R(N) (cm^{-1})	Obs-Calc (cm^{-1})	P(N) (cm^{-1})	Obs-Calc (cm^{-1})	R(N) (cm^{-1})	Obs-Calc (cm^{-1})	P(N) (cm^{-1})	Obs-Calc (cm^{-1})
0	1	...	...	22 463.7531	0.0203	...	...	...	...
	2	...	...	22 463.7962	0.0075	...	...	22 536.1069	0.0033
	3	22 466.0345	−0.0190	22 463.8735	0.0009	22 538.3453	−0.0166	22 536.1890	0.0021
	4	22 466.1535	−0.0120	22 463.9740	−0.0104	22 538.4563	−0.0228	22 536.2851	−0.0128
1	2	22 467.1588	−0.0037	22 462.8072	0.0066	22 539.4433	0.0033	22 535.1251	0.0020
	3	22 467.2456	−0.0008	22 462.8858	0.0013	22 539.5122	−0.0111	22 535.1971	−0.0093
	4	22 467.3586	0.0004	22 462.9987	0.0024	22 539.6308	−0.0035	22 535.3204	0.0030
2	2	22 468.4159	−0.0077	22 461.8870	0.0061	22 540.6840	0.0002	22 534.2178	0.0094
	3	22 468.5066	−0.0009	22 461.9689	0.0042	22 540.7583	−0.0088	22 534.2930	0.0013
	4	22 468.6165	−0.0028	22 462.0772	0.0007	22 540.8731	−0.0050	22 534.4074	0.0047
3	2	22 469.7476	−0.0055	22 461.0354	0.0061	22 541.9974	0.0040	22 533.3512	−0.0084
	3	22 469.8344	−0.0025	22 461.1108	−0.0024	22 542.0754	−0.0013	22 533.4505	0.0077
	4	22 469.9444	−0.0043	22 461.2281	0.0031	22 542.1967	0.0090	22 533.5516	−0.0022
4	2	22 471.1416	−0.0091	22 460.2414	−0.0047	22 543.3835	0.0147	22 532.5856	0.0091
	3	22 471.2350	0.0004	22 460.3251	−0.0048	22 543.4585	0.0064	22 532.6581	−0.0017
	4	22 471.3505	0.0041	22 460.4363	−0.0054	22 543.5697	0.0066	22 532.7687	−0.0021
5	2	22 472.6259	0.0092	22 459.5311	0.0000	22 544.8182	0.0081	22 531.8632	0.0039
	3	22 472.7130	0.0125	22 459.6109	0.0040	22 544.8952	0.0019	22 531.9404	−0.0021
	4	22 472.8239	0.0116	22 459.7231	0.0037	22 545.0028	−0.0015	22 532.0536	0.0001
6	2	22 474.1542	0.0033	22 458.8812	−0.0032	22 546.3217	0.0046	22 531.2090	0.0011
	3	22 474.2468	0.0120	22 458.9643	−0.0039	22 546.4007	0.0003	22 531.2895	−0.0016
	4	22 474.3517	0.0051	22 459.0750	−0.0050	22 546.5148	0.0034	22 531.4076	0.0055
7	2	22 475.7510	−0.0024	22 458.3146	0.0087	22 547.8966	0.0066	22 530.6270	0.0047
	3	22 475.8392	0.0020	22 458.3799	−0.0099	22 547.9811	0.0078	22 530.6891	−0.0165
	4	22 475.9585	0.0095	22 458.5003	−0.0013	22 548.0887	0.0045	22 530.8268	0.0103
8	2	22 477.4263	0.0022	22 457.7943	−0.0015	22 549.5367	0.0080	22 530.0937	−0.0088
	3	22 477.5093	0.0013	22 457.8828	0.0032	22 549.6079	−0.0040	22 530.1772	−0.0086
	4	22 477.6219	0.0021	22 457.9886	−0.0028	22 549.7307	0.0078	22 530.3033	0.0065
9	2	22 479.1543	−0.0089	22 457.3532	−0.0007	...	...	22 529.6396	−0.0090
	3	22 479.2440	−0.0030	22 457.4411	0.0034	22 551.3192	0.0027	22 529.7356	0.0038
	4	22 479.3594	0.0006	22 457.5510	0.0015	22 551.4248	−0.0027	22 529.8518	0.0090
10	2	22 480.9612	−0.0093	...	...	22 552.9873	−0.0163	...	...
	3	22 481.0583	0.0040	22 457.0692	0.0051	22 553.0823	−0.0045	...	...
	4	22 481.1646	−0.0015	22 457.1813	0.0054	22 553.1980	0.0002	22 529.4604	0.0057
11	2	22 482.8336	−0.0124			22 554.8317	−0.0080		
	3	22 482.9236	−0.0063			22 554.9181	−0.0049		
	4	22 483.0473	0.0056			22 555.0302	−0.0037		
12	2	22 484.7873	−0.0026			...	...		
	3	22 484.8734	−0.0003			22 556.8251	0.0002		
	4	22 484.9916	0.0061			22 556.9401	0.0042		
13	3	22 486.8860	0.0002						
	4	22 486.9978	0.0002						

TABLE IV. Equilibrium parameters of AlC in the ground and electronic excited states.

	$X\,^4\Sigma^-$ Ground state		$B\,^4\Sigma^-$ Excited state	
Parameter	Present expt.	Previous expt.[a]	Present expt.	Previous expt.[a]
B_e (cm^{-1})	0.530 668(78)	0.531 012(64)	0.565 149(70)	0.565 807(72)
α_e (cm^{-1})	0.005 00(10)	0.005 094(24)	0.006 23(9)	0.006 393(75)
r_e (Å)	1.955 7(1)	1.955 0	1.894 6(1)	1.893 9

[a]Reference 17.

smaller B_e values, obtained by fitting the rotational structure in a different manner.

It is striking that all of the calculations reported in Table I overestimate the ground state equilibrium bond length of AlC by 0.01–0.02 Å. In an effort to explore this deficiency, we used coupled cluster singles and doubles with triples added perturbatively (CCSD(T)) methods with large correlation consistent basis sets to predict the bond length (R_e) and

TABLE V. *Ab intio* calculations of the ground state bond length of AlC.

	$X^4\Sigma^-$ State bond length (Å)	
Basis set	CCSD(T)/valence	CCSD(T)/core
$n = 3$	1.9753[a]	1.9708[b]
$n = 4$	1.9674	1.9592
$n = 5$	1.9648	1.9568
CBS	1.9635	1.9562

[a]Basis set aug-cc-pVnZ on carbon, aug-cc-pV(n+d)Z on aluminum.
[b]Basis set aug-cc-pCVnZ on both atoms, see text.

extrapolated the results to the complete basis set limit using the simple exponential function,[39]

$$R_e(\mathrm{n}) = R_e(\mathrm{CBS}) + Ae^{-bn}, \quad (3)$$

where n is the basis set index with $n = 3$ for aug-cc-pVTZ, $n = 4$ for aug-cc-pVQZ, etc. The three parameters R_e(CBS), A, and b were exactly fit to the $n = 3$, 4, and 5 bond lengths to obtain the CBS extrapolated quantity. Initially, we used the aug-cc-pVnZ basis sets for carbon and the aug-cc-pV(n+d)Z basis sets for aluminum, correlating only the valence electrons. The results, given in Table V, show a steadily decreasing bond length with increasing size of the basis set, with a CBS value of 1.9635 Å, still 0.0078 Å larger than experiment. It has been repeatedly shown that the calculation of high-accuracy molecular geometries often requires that the core electrons also be correlated and Gaussian basis sets have been developed to provide a balanced description for all the electrons in such calculations.[40] To investigate core correlation effects, we have used the aug-cc-pCVnZ family of basis sets, which were developed specifically for this purpose, correlating both core and valence electrons except the very low-lying 1s electrons. The results and the extrapolation to the CBS limit are given in Table V. It is gratifying that a systematic application of higher levels of theory with larger and larger basis sets converges to a bond length that is only 0.0005 Å greater than the experimental value.

The previous theoretical prediction[25] of the B state equilibrium bond length was 1.916 Å, again somewhat larger than our value of 1.8946(1) Å, but the predicted change on electronic excitation of −0.055 Å is very close to the observed −0.061 Å diminution in the bond length. Molecular orbital theory satisfactorily accounts for this decrease in the bond length in the excited state.[20,25]

The excited state Fermi contact parameter obtained in the present work gives some insight into the nature of the σ molecular orbital containing the unpaired electron in the AlC electronic excited state. The predominant electron configuration for the ground state (valence electrons only) is $1\sigma^2 2\sigma^2 3\sigma^1 \pi_x^1 \pi_y^1$ where the 2σ orbital is primarily a 3s orbital on Al and the 3σ orbital is formed from the overlap of the carbon and aluminum 2p_z orbitals. The $B\,^4\Sigma^-$ excited state is formed primarily by promotion of an electron from the 2σ to the 3σ molecular orbital, with configuration $1\sigma^2 2\sigma^1 3\sigma^2 \pi_x^1 \pi_y^1$. Since only s electron wavefunctions have nonzero amplitude at the nucleus, the Fermi contact parameter is a measure of the unpaired s electron spin density, in this case involving the aluminum 3s electron. The percentage of Al 3s character in the 2σ orbital may be obtained by comparing the molecular Fermi contact parameter, b_F, to that of an electron in the aluminum atomic 3s orbital, b_F (Al 3s), via

$$\%3s = \frac{b_F(AlC)}{\frac{1}{3}b_F(Al\ 3s)} \times 100. \quad (4)$$

The factor of 1/3 appears because the single electron in the 2σ orbital is only one of three unpaired electrons in the $B\,^4\Sigma^-$ excited state.[41] Using the Morton and Preston[42] *ab initio* atomic value of b_F (Al 3s) = 3911 MHz (0.1305 cm^{-1}) yields 62.1% as the percentage of 3s character in the 2σ orbital, entirely consistent with the notion that the B state involves an aluminum 3s to carbon 2pσ charge transfer.[20]

VI. CONCLUSIONS

The present reevaluation of the small splittings in the spectrum of the AlC free radical is a result of slight improvements in resolution (0.05 cm^{-1} vs 0.1 cm^{-1}) over the previous study.[15] It is very clear that the structure in the rotational lines is due to the substantial aluminum Fermi contact interaction in the $B\,^4\Sigma^-$ electronic excited state. The derived equilibrium ground state bond length of 1.9557(1) Å is very satisfactorily reproduced by our high level *ab initio* calculations that include core correlation effects. The experimentally determined 0.06 Å decrease in the bond length on electronic excitation is precisely as expected from molecular orbital considerations. The determination of the small spin-spin splittings in the gas phase spectrum of aluminum carbide will have to await future higher resolution studies.

ACKNOWLEDGMENTS

We owe a debt of thanks to Mohammed Gharaibeh and Tim Little for early experimental forays into the spectroscopy of AlC in our laboratory. D.J.C. is very grateful for several illuminating discussions with Chris Brazier, Department of Chemistry and Biochemistry, California State University Long Beach, concerning the role of hyperfine interactions in the excited state of AlC. A.K. thanks the Graduate School of the University of Kentucky for the support of a Lyman T. Johnson Fellowship. This material is based upon work supported by the National Science Foundation under Grant No. CHE-1106338.

[1]J. Cernicharo, C. A. Gottlieb, M. Guelin, P. Thaddeus, and J. M. Vrtilek, Astrophys. J. **341**, L25 (1989).
[2]P. Thaddeus, S. E. Cummins, and R. A. Linke, Astrophys. J. **283**, L45 (1984).
[3]M. C. McCarthy, A. J. Apponi, and P. Thaddeus, J. Chem. Phys. **110**, 10645 (1999).
[4]M. Ohishi, N. Kaifu, K. Kawaguchi, A. Murakami, S. Saito, S. Yamamoto, S. Ishikawa, Y. Fujita, Y. Shiratori, and W. M. Irvine, Astrophys. J. **345**, L83 (1989).
[5]G. Pascoli and M. Comeau, Astrophys. Space Sci. **226**, 149 (1995).
[6]J. Cernicharo and M. Guelin, Astron. Astrophys. **183**, L10 (1987).
[7]L. M. Ziurys, A. J. Apponi, and T. G. Phillips, Astrophys. J. **433**, 729 (1994).
[8]L. M. Ziurys, C. Savage, J. L. Highberger, A. J. Apponi, M. Guelin, and J. Cernicharo, Astrophys. J. **564**, L45 (2002).
[9]E. D. Tenenbaum and L. M. Ziurys, Astrophys. J. **712**, L93 (2010).
[10]E. D. Tenenbaum and L. M. Ziurys, Astrophys. J. **694**, L59 (2009).
[11]A. Thoma, N. Caspary, B. E. Wurfel, and V. E. Bondybey, J. Chem. Phys. **98**, 8458 (1993).
[12]P. B. Zeeman, Can. J. Phys. **32**, 9 (1954).

[13]D. S. Ginter, M. L. Ginter, and K. K. Innes, Astrophys. J. **139**, 365 (1964).
[14]L. B. Knight, Jr., S. T. Cobranchi, J. O. Herlong, and C. A. Arrington, J. Chem. Phys. **92**, 5856–5866 (1990).
[15]C. R. Brazier, J. Chem. Phys. **98**, 2790 (1993).
[16]G. V. Chertihin, L. Andrews, and P. R. Taylor, J. Am. Chem. Soc. **116**, 3513 (1994).
[17]C. R. Brazier and M. A. Tandoc, J. Mol. Spectrosc. **258**, 42 (2009).
[18]A. V. Zaitsevskii, A. I. Dement'ev, and G. N. Zviadadze, J. Less-Common Met. **117**, 237 (1986).
[19]G. L. Gutsev, P. Jena, and R. J. Bartlett, J. Chem. Phys. **110**, 2928 (1999).
[20]C. W. Bauschlicher, Jr., S. R. Langhoff, and L. G. M. Pettersson, J. Chem. Phys. **89**, 5747 (1988).
[21]A. Largo, P. Redondo, and C. Barrientos, J. Phys. Chem. **106**, 4217 (2002).
[22]S. Midda and A. K. Das, J. Mol. Struct. **633**, 67 (2003).
[23]G. Li and Z. Tang, J. Phys. Chem. **107**, 5317 (2003).
[24]P. Redondo, C. Barrientos, and A. Largo, Int. J. Quantum Chem. **96**, 615 (2004).
[25]D. Tzeli and A. Mavridis, J. Phys. Chem. A **105**, 1175 (2001).
[26]D. Tzeli and A. Mavridis, J. Phys. Chem. A **105**, 7672 (2001).
[27]W. W. Harper and D. J. Clouthier, J. Chem. Phys. **106**, 9461 (1997).
[28]D. L. Michalopoulos, M. E. Geusic, P. R. R. Langridge-Smith, and R. E. Smalley, J. Chem. Phys. **80**, 3556 (1984).
[29]J. Yang and D. J. Clouthier, J. Chem. Phys. **135**, 054309 (2011).
[30]J. Cariou and P. Luc, *Atlas du Spectre d'Absorption de la Molecule de Tellure* (CNRS, Paris, 1980).
[31]M. J. Frisch, G. W. Trucks, H. B. Schlegel *et al.*, GAUSSIAN 09, Revision C.02, Gaussian, Inc., Wallingford, CT, 2004.
[32]A. D. Becke, J. Chem. Phys. **98**, 5648 (1993).
[33]C. Lee, W. Yang, and R. G. Parr, Phys. Rev. B **37**, 785 (1988).
[34]T. H. Dunning, Jr., K. A. Peterson, and A. K. Wilson, J. Chem. Phys. **114**, 9244 (2001).
[35]D. J. Feller, J. Comput. Chem. **17**, 1571 (1996).
[36]PGOPHER, a Program for Simulating Rotational Structure, C. M. Western, University of Bristol, http://pgopher.chm.bris.ac.uk.
[37]C. R. Brazier, private communication (2015).
[38]R. A. Frosch and H. M. Foley, Phys. Rev. **88**, 1337 (1952).
[39]D. Feller, K. A. Peterson, and J. G. Hill, J. Chem. Phys. **135**, 044102 (2011), and references therein.
[40]K. A. Peterson and T. H. Dunning, Jr., J. Chem. Phys. **117**, 10548 (2002).
[41]T. D. Varberg, R. W. Field, and A. J. Merer, J. Chem. Phys. **95**, 1563 (1991).
[42]J. R. Morton and K. F. Preston, J. Magn. Reson. **30**, 577 (1978).